

THE EXPANSION OF A CYLINDER UNDER CONDITIONS OF FINITE PLANE STRAIN

J.P. CARTER *

Engineering Department, Univeristy of Cambridge, Cambridge CB2 1PZ, England

Received 17 August 1977

The problem of the expansion of an initially thick-walled cylinder due to an internal pressure under conditions of plane strain is considered. The cylinder is composed of an elasto-plastic, Tresca material with an associated flow rule. No restriction is placed on the magnitude of the deformation or on the magnitude of the material parameters. Solutions are presented for a particular initial (stress free) geometry and it is shown that the maximum value of the internal pressure is a function of the deformation to strength parameter ratio.

1. Introduction

Much attention has been paid to the problem of the expansion of a cylinder due to internal pressure for both rigid plastic and elasto-plastic materials. For a survey of this work reference may be made to a text by Hill [1] and to papers by Hodge and White [2], Allen and Sopwith [3], Beliaev and Sinitzky [4] and Steele [5]. Koiter [6] gives a lucid description of the basic assumptions and results of most of these works as well as presenting an infinitesimal strain solution for a Tresca [7] material with an associated flow rule.

For a cylinder expanding under conditions of plane strain, the problem of unrestricted plastic flow has been dealt with by Prager and Hodge [8] using the von Mises [9] theory, and by Hill et al. [10] using a treatment based on the Prandtl–Reuss [11,12] theory. The former approach assumes that the material is incompressible and neglects elastic strains in the plastic region, while the latter includes an account of the elastic component of strain but assumes that changes in geometry are small. It is the aim of this paper to solve the problem of unrestricted flow for a material with a Tresca yield criterion and an associated flow rule. The present analysis applies to materials possessing deformation moduli of any magnitude, including the less stiff. That is to say that no restriction is placed

on the elastic component of strain or the magnitude of the overall deformation. Exact equations governing the finite deformation behaviour are formulated and these are solved approximately using a numerical technique.

2. Governing equations

A general method of analysis for the problem of finite elasto-plastic deformation has been presented by Carter et al. [13]. This analysis will be applied to the problem described in fig. 1. For the case of plane strain cylinder expansion the use of symmetry allows simplifications to be made to the general equations governing finite deformation.

Consider a typical particle of the deforming cylinder to be located at time t_0 at a distance r_0 from its centre O . At some later time t this material particle occupies a position which is a distance r from O . From symmetry we see that displacement may occur only in the radial direction. This change in location $u = r - r_0$ is a result of an increase in internal pressure from p_0 to p during the time interval (t_0, t) . The radial velocity of the particle at time t is given by

$$v = \frac{\partial u}{\partial t}(r_0, t) = \frac{du}{dt}(r, t). \quad (1)$$

Since there are no rotations and no radial or tangential shear deformations associated with the expansion, a

* Formerly: Department of Civil Engineering, University of Sydney, Australia.

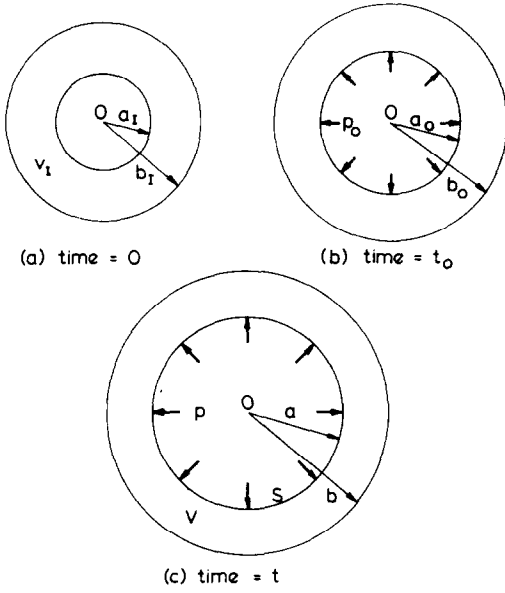


Fig. 1. Cylinder expansion.

complete description of the deformation is given, in Eulerian terms, by the vector of rate quantities

$$\boldsymbol{\varepsilon}^T = \left(\frac{\partial v}{\partial r}, \frac{v}{r} \right). \quad (2)$$

A description of the stress field at r , at time t , is also given by

$$\boldsymbol{\sigma}^T = (\sigma_{rr}, \sigma_{\theta\theta}), \quad (3)$$

where σ_{rr} and $\sigma_{\theta\theta}$ are the radial and tangential normal stress components, respectively, and tensile stresses are reckoned positive.

We assume that the material of the cylinder obeys a general rate law given by

$$\dot{\boldsymbol{\sigma}} = D\boldsymbol{\varepsilon}, \quad (4)$$

where the dot indicates material differentiation with respect to time (in the absence of rotations $\dot{\boldsymbol{\sigma}}$ provides an objective measure of the stress rate and there is no need to employ a more general measure such as that due to Jaumann [14]). For an elastic material the matrix D is given by

$$D = \begin{pmatrix} \Lambda + 2G & \Lambda \\ \Lambda & \Lambda + 2G \end{pmatrix}, \quad (5)$$

where Λ and G are the Lamé parameters of the classical theory of elasticity.

This material yields according to the Tresca criterion which may be written

$$\sigma_1 - \sigma_3 = 2c, \quad (6)$$

where $\sigma_1 > \sigma_2 > \sigma_3$ (tension positive) are the principal stresses and c is the yield limit in pure shear. We assume, without proof, that in this problem $\sigma_1 = \sigma_{\theta\theta}$, $\sigma_3 = \sigma_{rr}$, and that the intermediate principal stress σ_2 is the axial stress component σ_{xx} . This is not an unreasonable assumption for the solutions presented later. Koiter [6] has shown that it is in fact valid for the small strain theory when the initial value of the ratio of external to internal radii, b_1/a_1 , is less than 5.75. We note also that it is valid in the other extreme, i.e. the finite strain solution for a material that remains elastic.

Once yielding has occurred the cylinder material flows plastically according to an associated flow law and the matrix D is then given by

$$D = (\Lambda + G) \begin{pmatrix} 1 & 1 \\ 1 & 1 \end{pmatrix}. \quad (7)$$

Integration of eq. (4) with respect to time gives

$$\boldsymbol{\sigma} = \int_{t_0}^t D\boldsymbol{\varepsilon} dt + \boldsymbol{\sigma}_0, \quad (8)$$

where $\boldsymbol{\sigma}_0$ is the vector of stress components at r_0 at time t_0 .

We may replace the equation of total equilibrium by the virtual work expression which, in the absence of body-forces, may be written

$$\int_V d\boldsymbol{\varepsilon}^T \boldsymbol{\sigma} dV = \int_S dv p dS, \quad (9)$$

where V is the cross-section of the cylinder and S its inner surface at time t . The outer surface remains stress free. The incremental velocity dv is compatible with the incremental deformation rates $d\boldsymbol{\varepsilon}$ and the velocity boundary conditions on the inner cylindrical surface.

Substitution of eq. (8) into the virtual work expression gives

$$\int_V d\boldsymbol{\varepsilon}^T \left\{ \int_{t_0}^t D\boldsymbol{\varepsilon} dt \right\} dV = \int_S dv p dS - \int_V d\boldsymbol{\varepsilon}^T \boldsymbol{\sigma}_0 dV. \quad (10)$$

Because V and S are changing with time it is generally impossible to solve eq. (10) exactly and an approximate numerical solution is necessary.

3. Numerical solution

An approximate solution for the displacement and stress fields u and σ can be obtained using the finite element technique for spatial integration in eq. (14).

Because of symmetry we focus attention on only one radial line of the cylinder. If such a continuous line is divided into a discrete number of conforming elements then suppose that the displacement field u can be adequately represented by values at the connecting nodes 1, 2, ..., N and let

$$\Delta \delta^T = (u_1, u_2, \dots, u_N) = \delta^T(t) - \delta_0^T(t), \quad (11)$$

where $\delta^T(t)$ is the vector of total nodal displacements in the time interval $(0, t)$. The subscripts in eq. (11) refer to the node numbers.

Suppose that the continuous velocity field can be approximated by

$$v = A \Delta \dot{\delta} = A \dot{\delta}, \quad (12)$$

where the form of A will depend upon the particular type of element used and will, in general, depend upon its current position. It follows then that the vector of deformation rates may be related to $\dot{\delta}$ by the approximation

$$\epsilon = B \dot{\delta}, \quad (13)$$

where

$$B = \begin{pmatrix} \partial/\partial r \\ 1/r \end{pmatrix} A.$$

Substituting into eq. (10) it is found that for arbitrary variations $\Delta \dot{\delta}$ consistent with the velocity boundary conditions

$$\begin{aligned} \Delta \dot{\delta}^T \int_V B^T \left\{ \int_{t_0}^t DB \dot{\delta} dt \right\} dV \\ = \Delta \dot{\delta}^T \int_S p \eta dS - \Delta \dot{\delta}^T \int_V B^T \sigma_0 dV, \end{aligned} \quad (14)$$

and thus that

$$\int_V B^T \left\{ \int_{t_0}^t DB \dot{\delta} dt \right\} dV = \int_S p \eta dS - \int_V B^T \sigma_0 dV, \quad (15)$$

where $\eta^T = (1, 0, \dots, 0)$ with N terms.

This finite element equation is an integral equation in time and an approximate solution may be obtained by following a load path using a number of finite but small steps. For any such step in time Δt we approximate all time-dependent quantities by their average values for this particular step. Eq. (16) then reduces to the approximate set of equations

$$\bar{K} \Delta \delta = \bar{f}, \quad (16)$$

where

$$\bar{K} = \frac{\int_V B^T DB dV}{\bar{V}}$$

and

$$\bar{f} = \frac{\int_S p \eta dS}{\bar{V}} - \frac{\int_V B^T \sigma_0 dV}{\bar{V}}.$$

The bar denotes some average or representative value of the quantity for the current time step and the integrations are performed over the 'mean' configuration. Iteration may thus be necessary within each time step. In this manner spatial and time integrations are performed simultaneously to obtain the time-varying domain V . The solution at any time t is completed by integration of the constitutive equations (4) to obtain the stress field σ within V .

4. The cylinder solutions

The numerical technique described above was applied to the expansion of a cylinder the finite element idealization of which is shown in fig. 2. The mesh is shown at the stress-free configuration at time $t = 0$ when $b_1/a_1 = 2$.

In addition there are two closed form solutions to this problem that are, strictly speaking, applicable only under certain circumstances.

(a) A solution reported by Hill [1] and Koiter [6] and strictly applicable only when $G/c = \infty$. This is the

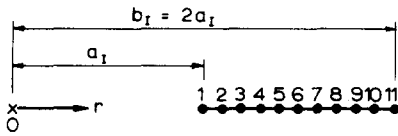


Fig. 2. Finite element mesh at $t = 0$.

conventional small strain solution that does have practical application for materials of high deformation modulus. According to this theory the maximum internal pressure, p_H , which is determined by complete yield within the cylinder is given by

$$p_H/c = 2 \ln(b_I/a_I). \tag{17}$$

(b) A solution for materials of infinite strength (i.e. $G/c = 0$) is presented in the Appendix and the current value of the outer radius b is plotted against the internal pressure in fig. 3 for the case when Poisson's ratio, $\nu = 0.3$. For $G/c = 0$ the maximum pressure, p_c , which corresponds to elastic instability is given by

$$p_c/G = 2 \ln(b_I/a_I). \tag{18}$$

We thus note the interesting result that

$$p_c/p_H = G/c. \tag{19}$$

A solution for the material with $G/c = 0$ was also obtained using the numerical technique described above and numerical displacement results are compared with the rigorous solution in fig. 3. The elastic dilatation that is a consequence of adopting the material rate law of eq. (4) is evident from fig. 4, where the volume is plotted as a function of the outer radius (V_t, V are the cross-sectional areas at times 0 and t).

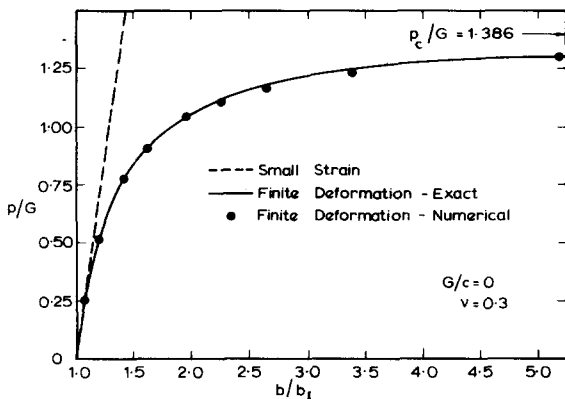


Fig. 3. Elastic cylinder expansion.

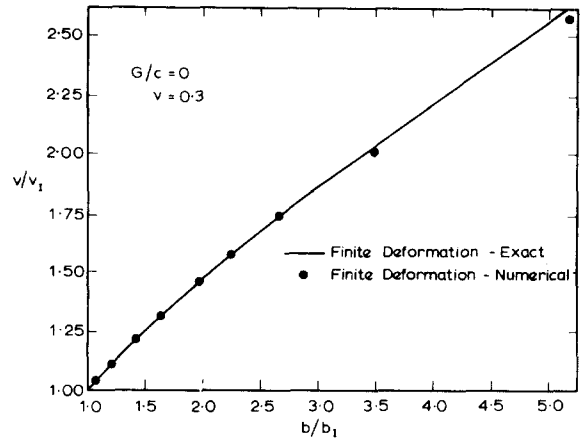


Fig. 4. Elastic cylinder - volume behaviour.

Neither of the closed form solutions (a) and (b) are strictly applicable to real materials as these possess finite values of G/c . However, either may provide adequate predictions of the behaviour of cylinders made from many materials in engineering use.

An examination of the behaviour of materials with a variety of G/c values has been made using the numerical technique described above. The relationship between the outer radius and the internal pressure for cylinders with $\nu = 0.3$ is plotted in fig. 5. Note that for stiffer materials, e.g. $G/c \geq 38.5$, the closed form solution (a) gives a very good approximation to the

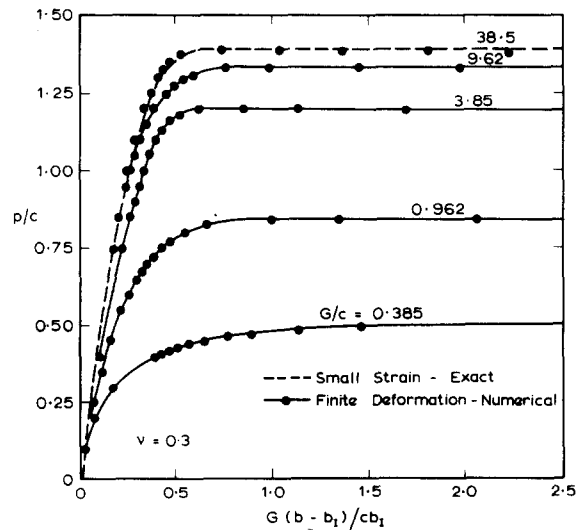


Fig. 5. Elasto-plastic cylinder behaviour.

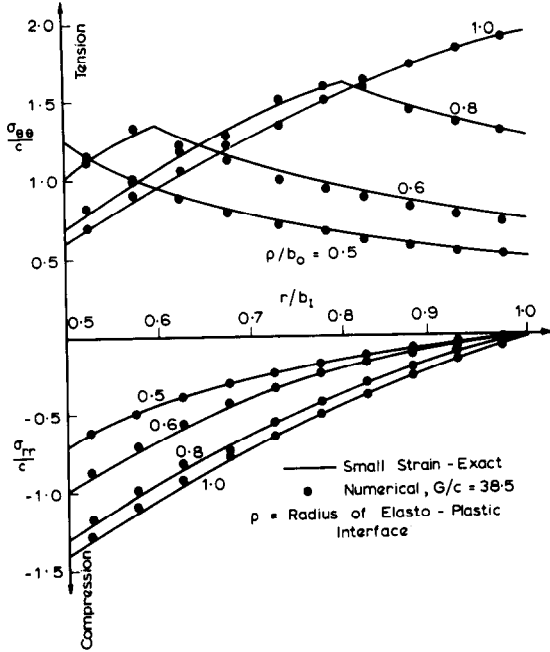


Fig. 6. Comparison of stress distributions.

expansion behaviour. The stresses obtained for the case of $G/c = 38.5$ are shown in fig. 6 to be in close agreement with those of the closed form solution. For less stiff materials the elasto-plastic behaviour becomes more like that predicted by the analytic method (b). The curve for $G/c = 0$ has no unique position on fig. 5 because the ordinate is plotted as p/c , but it is noted that for values of G/c less than about 0.385 the elasto-plastic behaviour is almost identical with that pre-

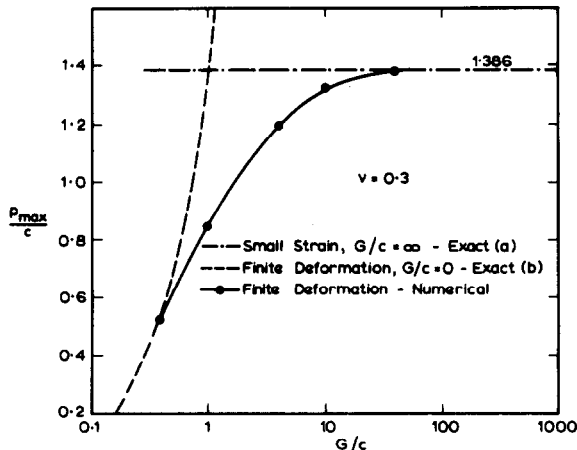


Fig. 7. Maximum pressure vs. material properties.

dicted by method (b) – at least for the range of displacements plotted. This may not continue to be the case when the cylinder expands further to become one with very thin walls.

The relationship between the maximum pressure, p_{max} , and the material properties is given in fig. 7. As G/c is increased p_{max} approaches the value predicted by method (a), while for lower values of G/c the limiting value is that of p_c , the elastic instability pressure.

Acknowledgement

The author would like to acknowledge the support of an Australian Commonwealth Post-Graduate Research Scholarship.

Appendix: elastic cylinder expansion

Consider the cylinder of fig. 1(c) which had the initial (stress free) configuration shown in fig. 1(a). We examine here the particular case of a cylinder composed of a material possessing infinite strength ($G/c = 0$). For an infinitesimal change in the pressure dp , the outer and inner radii change by amounts db and da , respectively, where from the elastic small strain theory we have

$$db = \left\{ \frac{2(1 - \nu^2)b}{(b/a)^2 - 1} \right\} \left(\frac{dp}{E} \right), \tag{A.1}$$

$$da = \left\{ \frac{1 + \nu}{(b/a)^2 - 1} \right\} \left\{ (1 - 2\nu)a + \frac{b^2}{a} \right\} \left(\frac{dp}{E} \right). \tag{A.2}$$

Let the parameter $R = b/a$. Then, on combination of eqs. (A.1) and (A.2) we obtain

$$dR/R = -2dp/G, \tag{A.3}$$

whence

$$R = R_1 e^{-2p/G}, \tag{A.4}$$

where

$$R_1 = b_1/a_1.$$

The maximum pressure, p_c will occur when $R = 1$, i.e.

$$(p_c/G) = 2 \ln R_1 \tag{A.5}$$

Current values of radii a and b at the pressure p are then given by

$$\ln \left[\frac{a}{a_1} \right] = \frac{1}{2} \left\{ (1 - 2\nu) \ln \left[\frac{(R/R_1)^2}{(1 - R^2)/(1 - R_1^2)} \right] - \ln \left[\frac{1 - R^2}{1 - R_1^2} \right] \right\}, \tag{A.6}$$

$$\ln \left[\frac{b}{b_1} \right] = \ln \left[\frac{R}{R_1} \right] + \ln \left[\frac{a}{a_1} \right]. \quad (\text{A.7})$$

References

- [1] R. Hill, *Mathematical theory of plasticity* (Oxford, 1950).
- [2] P.G. Hodge and G.N. White, *J. Appl. Mech.* 17 (1950) 180.
- [3] D.N. de G. Allen and D.G. Sopwith, *Proc. Roy. Soc. London, Ser. A* 205 (1951) 69.
- [4] N.M. Beliaev and A.K. Sinitsky, *Isvestia Akad. Nauk SSSR* 2 (1938) 3.
- [5] M.C. Steele, *J. Appl. Mech.* 19 (1952) 133.
- [6] W.T. Koiter, *On partially plastic thick-walled tubes* (Biezeno Anniversary Volume in Applied Mechanics, N.V. De Technische Uitgeverij H. Stam, Haarlem, 1953) p. 232.
- [7] H. Tresca, *Compt. Rend. Acad. Sci. Paris* 59 (1864) 754; 64 (1867) 809.
- [8] W. Prager and P.G. Hodge, *Theory of Perfectly Plastic Solids* (Wiley, New York, 1951).
- [9] R. von Mises, *Göttinger Nachrichten, Math.-phys. Klasse* (1913) 582.
- [10] R. Hill, E.H. Lee and S.J. Tupper, *Proc. Roy. Soc. London, Ser. A* 191 (1947) 278.
- [11] L. Prandtl, *Proc. 1st Int. Congr. Appl. Mech., Delft* (1924) 43.
- [12] A. Reuss, *Z. Angew. Math. Mech.* 10 (1930) 266.
- [13] J.P. Carter, J.R. Booker and E.H. Davis, *Int. J. Numer. Anal. Methods Geomech.* 1 (1977) 25.
- [14] G. Jaumann, *Sitzungsberichte Akad. Wiss., Wien (IIa)* (1911) 120, 385; see also *Grundlagen der Bewegungslehre* (Leipzig, 1905).